

This article was downloaded by:

On: 25 January 2011

Access details: *Access Details: Free Access*

Publisher *Taylor & Francis*

Informa Ltd Registered in England and Wales Registered Number: 1072954 Registered office: Mortimer House, 37-41 Mortimer Street, London W1T 3JH, UK



Separation Science and Technology

Publication details, including instructions for authors and subscription information:

<http://www.informaworld.com/smpp/title~content=t713708471>

Analysis of Ternary Distillation Column Sequences

Liem Dug Vu^a, Prashant B. Gadkari^a, Rakesh Govind^a

^a Department of Chemical & Nuclear Engineering, University of Cincinnati, Cincinnati, Ohio

To cite this Article Vu, Liem Dug , Gadkari, Prashant B. and Govind, Rakesh(1987) 'Analysis of Ternary Distillation Column Sequences', *Separation Science and Technology*, 22: 7, 1659 – 1690

To link to this Article: DOI: 10.1080/01496398708058428

URL: <http://dx.doi.org/10.1080/01496398708058428>

PLEASE SCROLL DOWN FOR ARTICLE

Full terms and conditions of use: <http://www.informaworld.com/terms-and-conditions-of-access.pdf>

This article may be used for research, teaching and private study purposes. Any substantial or systematic reproduction, re-distribution, re-selling, loan or sub-licensing, systematic supply or distribution in any form to anyone is expressly forbidden.

The publisher does not give any warranty express or implied or make any representation that the contents will be complete or accurate or up to date. The accuracy of any instructions, formulae and drug doses should be independently verified with primary sources. The publisher shall not be liable for any loss, actions, claims, proceedings, demand or costs or damages whatsoever or howsoever caused arising directly or indirectly in connection with or arising out of the use of this material.

Analysis of Ternary Distillation Column Sequences

LIEM DUC VU, PRASHANT B. GADKARI, and RAKESH GOVIND*

DEPARTMENT OF CHEMICAL & NUCLEAR ENGINEERING
UNIVERSITY OF CINCINNATI
CINCINNATI, OHIO 45221

Abstract

Eight complex distillation column configurations for a ternary feed mixture are modeled and studied. A modified complex method is used to minimize the cost of the configurations. Optimum regions for each configuration depending on the feed composition are derived. The result provides guidelines for the synthesis of distillation column configurations.

INTRODUCTION

In general, distillation column configurations can be classified into three generic types:

1. Conventional configurations—consisting of columns (with one condenser and one reboiler) which perform perfect splits or sharp separations between the components in the feed mixture.
2. Complex configurations—consisting of columns (each with one condenser and one reboiler) which perform nonsharp separations between the components.
3. Thermally coupled configurations—consisting of columns which are thermally integrated and do not necessarily have one condenser and one reboiler for each column.

Most previous studies, summarized in the next section, have concentrated on conventional configurations. The objective of this research

*To whom correspondence should be addressed.

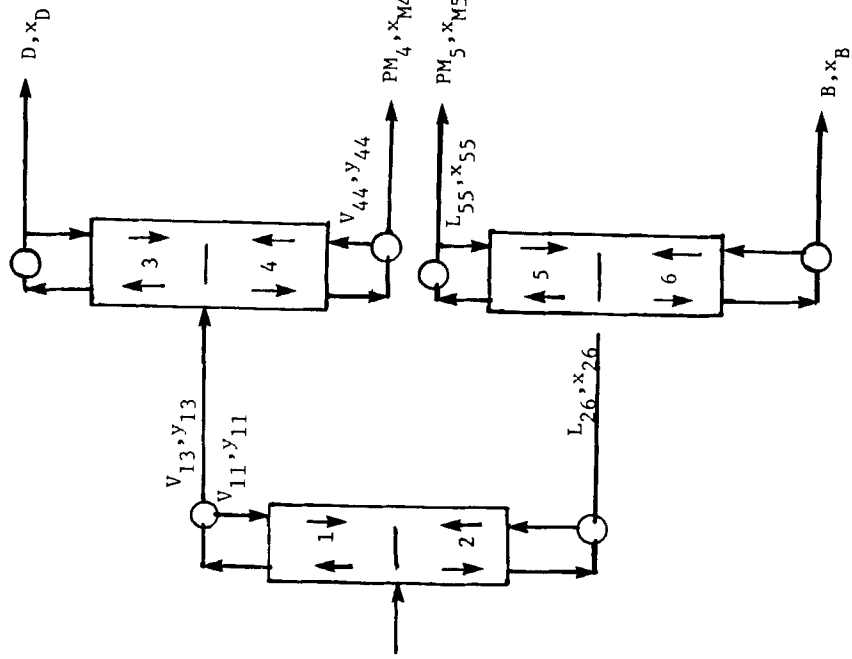


FIG. 1a. Configuration 1 for ternary mixture separation.

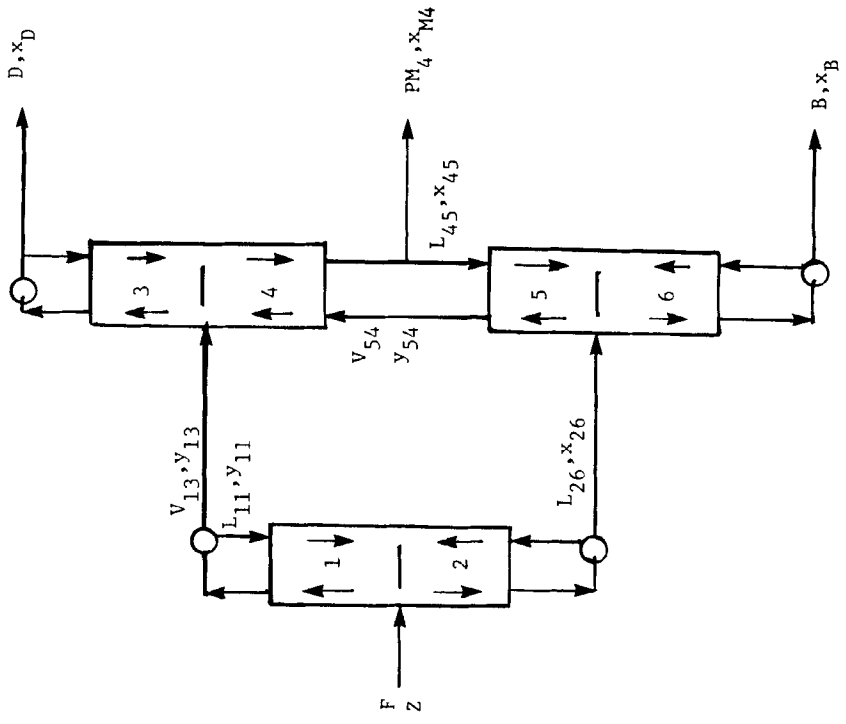


Fig. 1b. Configuration 2 for ternary mixture separation.

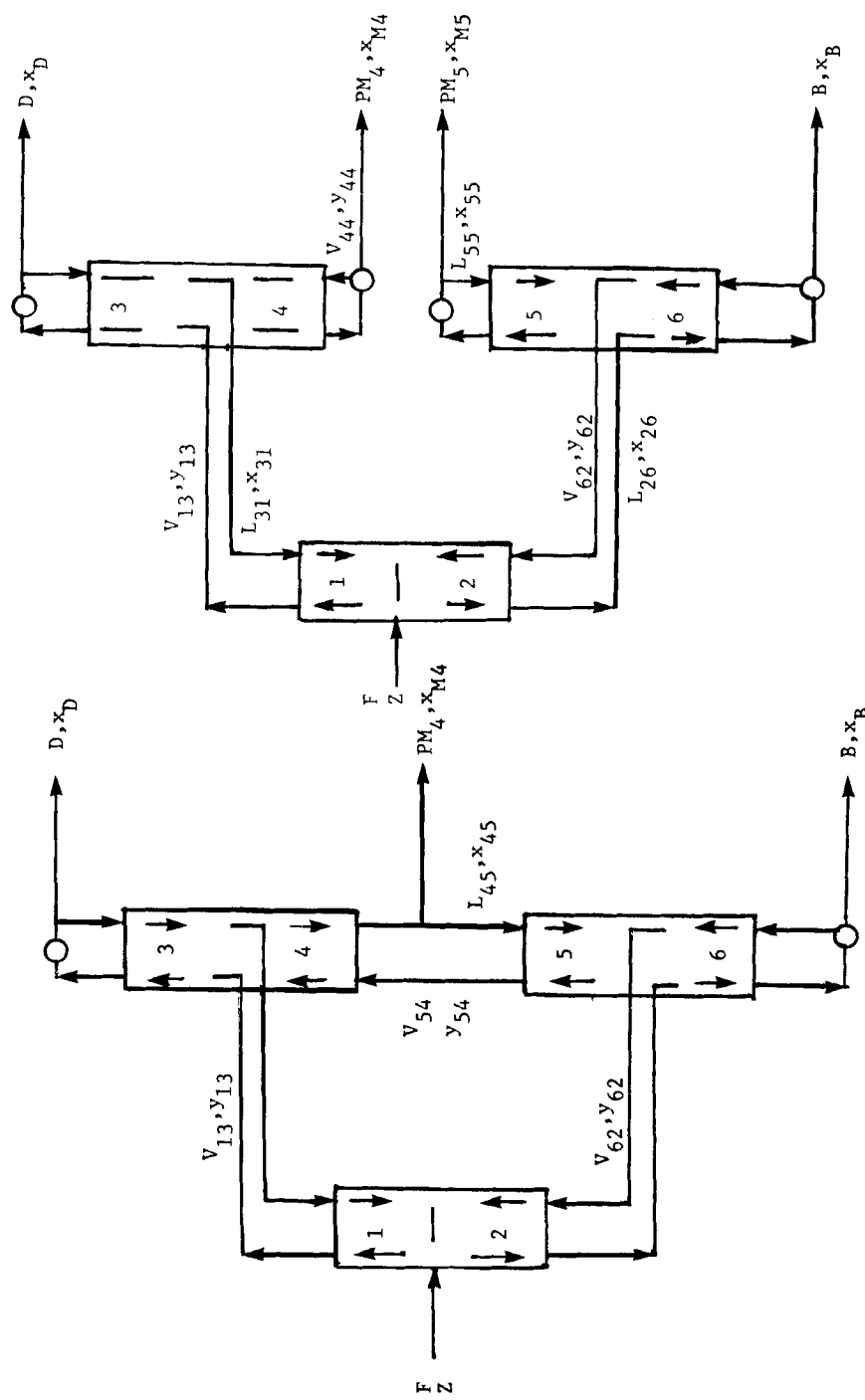


FIG. 1c. Configuration 3 for ternary mixture separation.

FIG. 1d. Configuration 4 for ternary mixture separation.

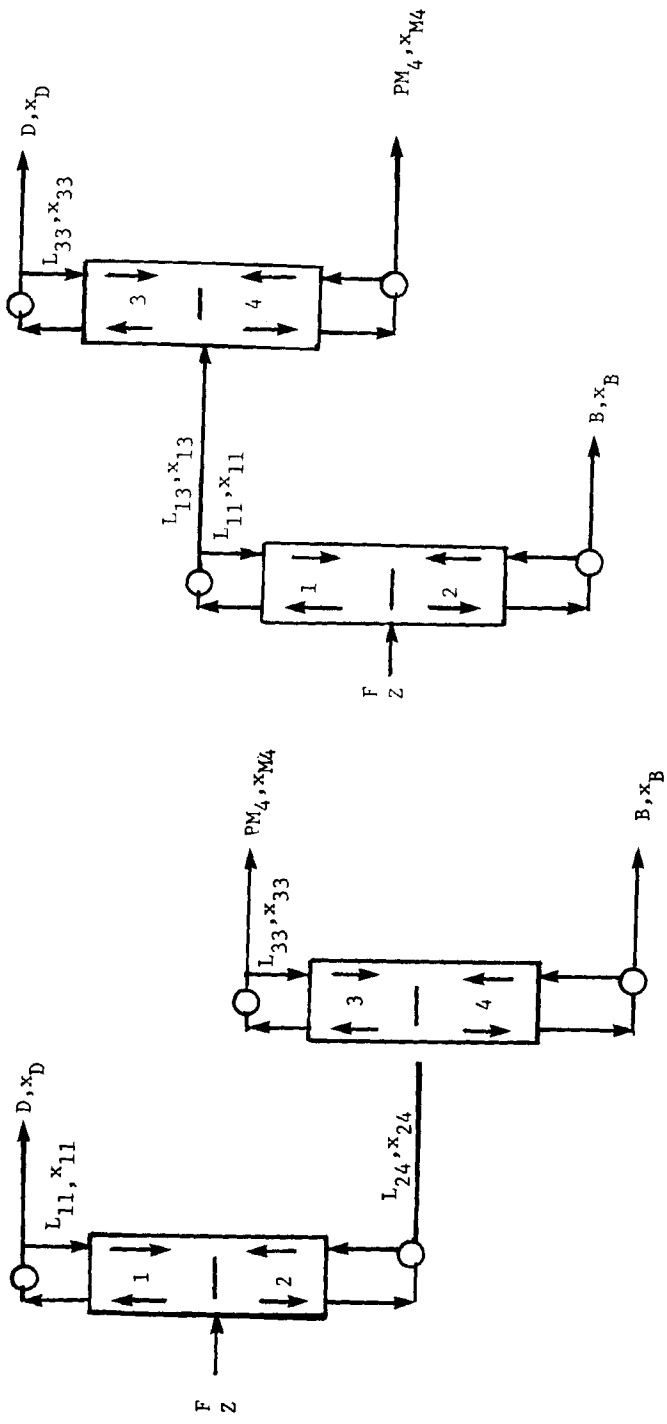


FIG. 1e. Configuration 5 for ternary mixture separation.

FIG. 1f. Configuration 6 for ternary mixture separation.

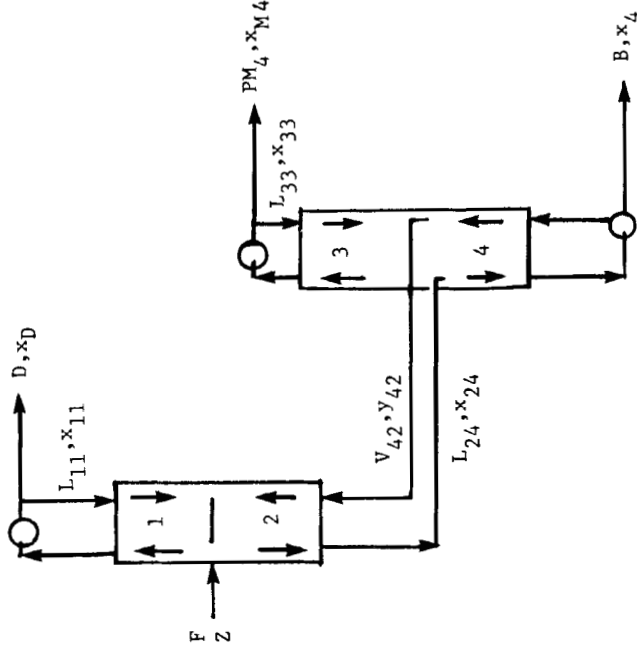


FIG. 1g. Configuration 7 for ternary mixture separation.

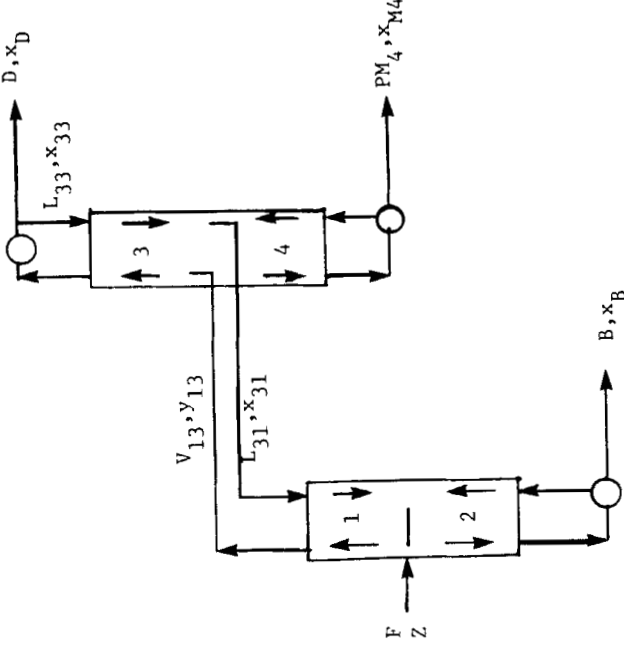


FIG. 1h. Configuration 8 for ternary mixture separation.

was to optimize the three types of configurations described above for a ternary feed mixture. Eight general configurations, shown in Figs. 1a-1h, are considered in this study. In this study the total cost of a configuration did not include the cost of the control structures, and in fact some of the structures would be difficult to control. The controllability of the structures was not investigated in this study.

Figures 1e and 1f show conventional configurations where pure products are removed sequentially using perfect splits in each column. The structures follow the rule that for an N component system, $(N - 1)$ distillation columns or $2(N - 1)$ countercurrent sections will be required to get all the pure products. (Each conventional column will be viewed as consisting of two countercurrent sections—one rectifying and one stripping.)

Figures 1a and 1b show complex configurations and these violate the $(N - 1)$ columns or $2(N - 1)$ sections rule which are valid for conventional configurations.

Figures 1c, 1d, 1g, and 1h show thermally coupled configurations in which energy is transferred between the columns by directly contacting the vapor and liquid streams. The structures might violate the $(N - 1)$ columns or $2(N - 1)$ section rule. In addition, each column is not restricted to one condenser and one reboiler.

BACKGROUND

The background for distillation configuration synthesis has been extensively reviewed by Nishida et al. (1). Some of the more relevant and recent work is briefly summarized below.

Petlyuk, Platonov, and Slavinskii (2) proposed and analyzed four schemes consisting of thermally coupled and complex configurations for a ternary feed mixture. The vapor feed ratio was used to compare among proposed schemes and two conventional configurations. Constant relative volatilities, constant liquid and vapor rates, and a liquid feed were assumed in the study. The authors studied five configurations. Four of them were identical to Configurations 1, 2, 3, and 4 analyzed in this paper. Their fifth configuration was a single tower with one feed and three products from the top, bottom, and intermediate tray in the column.

Stupin and Lockhart (3) used a case study to analyze one typical thermally coupled distillation system and compared it with two conventional schemes for one equimolar ternary feed mixture. Results showed that the thermally coupled system was favorable from the energy

conservation objective. The configurations discussed in their study are identical to Configurations 3, 5, and 6 in this paper.

Doukas and Luyben (4) studied the separation of a three-component feed in detail, with economic evaluation to compare two complex distillation systems with conventional schemes. The pressure in all columns was assumed to be atmospheric, and feeds with small compositions of intermediate component were not examined.

The configurations analyzed were the conventional direct and indirect sequences (Configurations 5 and 6 in this study) and Configuration 8 of this study. They also studied the single tower structure of Petlyuk et al. (2) with the side withdrawal product being a liquid stream.

Tedder and Rudd (5) used minimum venture cost to compare eight distillation systems (consisting of complex, thermally coupled, and conventional types) separating ternary feeds. Rules of thumb were discovered by studying optimum systems as functions of feed composition and relative volatilities. Four of the structures studied were identical to Configurations 1, 2, 5, and 6 of this study. Of the remaining four structures, two were identical to the single tower structure of Petlyuk et al. (2), one with side withdrawal below the feed and the other with side withdrawal above the feed. The remaining two structures were similar but not identical to Configurations 7 and 8 of this study. In their study the feed was introduced into the second column of Configurations 7 and 8 of this study.

Munoz and Seader (6) addressed the synthesis problem by means of thermodynamic objective functions. The objective function was defined in terms of the thermodynamic minimum work of separation. A thermodynamic search algorithm was proposed for the synthesis of separation sequences, both simple and complex. The configurations studied were identical to Configurations 1, 2, 5, and 6 in this study.

Recently, Fidkowski and Krolikowski (7) carried out an optimization of the thermally coupled Configuration 3. The objective function to be minimized was the minimum vapor flow rate from the system's reboiler required for the necessary separation. The optimization task was formulated as a nonlinear problem. Optimum values of decision variables and the optimum value of the objective function were found in the form of analytical expressions.

It is important to emphasize that optimal regions for Configurations 7 and 8 have not been presented in the literature.

ANALYSIS OF SEQUENCES

Component Distribution Calculation

In binary systems, if the feed composition Z_i and top product composition $X_{D,i}$ are specified, then the bottom product composition $X_{B,i}$

can have any desired value, and the material balance equations determine the flows of top and bottom products (*D* and *B*).

For multicomponent mixture distillation, this freedom of choice does not apply (8); often, considering feed compositions, the nature of feed, and the operating pressure, there remain only four variables that may be selected. If the reflux ratio is fixed and the optimum feed position is chosen, then only two variables are left. Thus, the complete compositions cannot be defined for either product stream. Hence, there is an unavoidable trial and error process that has to be made in the design calculations. Two methods are found useful for the above calculation. One is trial and error, using linear interpolation (applies for nonsharp separation cases), and the other is an analytical method for sharp separation cases.

For nonsharp separation cases the Petlyuk method (2) was used. The method is as follows:

Assume bottom product compositions, and calculate the top product compositions as

$$d_i = f_i - b_i \quad (1)$$

where d_i is component *i* flow rate in distillate product

b_i is component *i* flow rate in bottom product

f_i is component *i* flow rate in feed

With the bottom and top product compositions, the stage-to-stage calculations are carried out from the bottom up and the top down to the feed stage.

The disagreement of the intermediate components at the feed stage is calculated as

$$\delta_i = \frac{X_i^{\text{rect}} - X_i^{\text{strip}}}{X_i^{\text{rect}}}, \quad i = 2, \dots, N-1 \quad (2)$$

where X_i^{rect} is the liquid mole fraction at the feed stage calculated from the rectifying section calculation, and X_i^{strip} is the liquid mole fraction at the feed stage calculated from the stripping section calculation.

A correction is subsequently applied, calculated from linear interpolation as

$$b_i^k = b_i^k - \delta_i^{k-1} \frac{b_i^{k-1} - b_i^{k-2}}{\delta_i^{k-1} - \delta_i^{k-2}} \quad (3)$$

where k is the k th trial.

The calculation is repeated until δ_i converges to the tolerance range.

For sharp-separation cases, Yaws et al. (9) proposed an analytical method using Hengstebeck (10) and Geddes (11) equations. This method gives accurate predictions and is convenient to use.

The recovery of Component i in the distillate product is calculated as

$$\frac{d_i}{f_i} = \frac{10^{C_1} \alpha_i^{C_2}}{1 + 10^{C_1} \alpha_i^{C_2}} \quad (4)$$

and in the bottom product, it is

$$\frac{b_i}{f_i} = 1 - \frac{d_i}{f_i} = \frac{1}{1 + 10^{C_1} \alpha_i^{C_2}} \quad (5)$$

where the correlation constants C_1 and C_2 are calculated as

$$C_1 = -\log \frac{(b_{HK}/f_{HK})}{1 - (b_{HK}/f_{HK})} \quad (6)$$

$$C_2 = \frac{\log \left[\left(\frac{d_{LK}/f_{HK}}{1 - (d_{LK}/f_{LK})} \right) \left(\frac{b_{HK}/f_{HK}}{1 - (b_{HK}/f_{HK})} \right) \right]}{\log \alpha_{LK}} \quad (7)$$

where α is the relative volatility, and LK and HK are light key and heavy key, respectively. These components are adjacent components.

Stage to stage calculation (often called the Lewis-Matheson method) is used to determine the number of stages required. The equations used for costing the columns were the same as those used by Rathors et al. (12). Tables 1, 2, and 3 summarize the cost parameters used in this work.

The assumptions made in model development are as follows:

- (1) Constant molal overflows in all columns.
- (2) 99% recoveries for extreme components in relative volatilities where nonsharp separation occurs.
- (3) The thermally coupled liquids and vapors are acting as a partial condenser or reboiler where they are appropriate.
- (4) The mixture follows Raoult's law.
- (5) All products are bubble point liquid streams.
- (6) Constant pressure for each column; no pressure drop between stages.

TABLE I
Cost Parameters Used in This Work

Material of construction: carbon steel

Column instrumentation cost: \$4,000.00

Maintenance cost of the column (13): 2% of total installed cost of the column

Cost of utilities (13):

Utilities	Cost (\$/million kcal)
Steam (28.23 atm)	4.29
Steam (4.08 atm)	2.40
Steam (1.70 atm)	1.75
Cooling water (32.2°C)	0.28
Ammonia (1°C)	6.91
Ammonia (-17.78°C)	12.43
Ammonia (-21.67°C)	16.59

Physical properties: Enthalpies values estimate obtained from Maxwell (14) and correlated into function of P and T by nonlinear regression program, see Table 2. A_1 , A_2 , and A_3 are Antoine's constants obtained from Henley and Seader (15), see Table 3.

Assumed values: $\eta = 80\%$ efficiency for all trays; $H_r = 8500$, operating hours per year; project life = 10 years.

(7) Problem specifications are: feed composition, nature of feed, and recoveries of components in products.

Determining the optimum is a two-level optimization problem. It consists of optimizing individual column performance in the configuration and optimizing the configuration as a whole.

For one typical configuration the material balance equations used for modeling are shown in Fig. 2. Material balance equations for the other configurations can be obtained in a similar manner.

OPTIMIZATION PROCEDURE

The modified complex method (16) has been used for optimizing column configurations. It is a direct search method, and only requires the iterative computations of the design calculations without finding any

TABLE 2
Vapor and Liquid Enthalpy Data for *n*-Pentane, *n*-Hexane, and *n*-Heptane

	<i>n</i> -Pentane	<i>n</i> -Hexane	<i>n</i> -Heptane
<i>d</i> ₀	6223.966	8583.119	8569.127
<i>d</i> ₁	8.615	2.353	9.401
<i>d</i> ₂	0.0352	0.05221	0.05081
<i>d</i> ₃	-147.902	-161.644	-210.363
<i>d</i> ₄	0.21346	0.2294	0.2594

Liquid Enthalpy

$$h = e_0 + e_1T + e_2T^2$$

assume $h \neq f(P)$ where h = kcal/kg · mol, T = °K

	<i>n</i> -Pentane	<i>n</i> -Hexane	<i>n</i> -Heptane
<i>e</i> ₀	-3325.46	-3410.59	-3583.996
<i>e</i> ₁	16.661	16.869	17.016
<i>e</i> ₂	0.0436	0.05331	0.063

TABLE 3
Antoine's Constants for *n*-Pentane, *n*-Hexane, and *n*-Heptane

Antoine equation for vapor pressure:

$$\log P^\circ = A_1 - \frac{A_2}{T + A_3}$$

where P° = atm, T = °K

	<i>n</i> -Pentane	<i>n</i> -Hexane	<i>n</i> -Heptane
<i>A</i> ₁	4.06418	4.0984	4.0307
<i>A</i> ₂	1109.2505	1226.8437	1273.4361
<i>A</i> ₃	-36.2528	-42.5588	-55.4843

$$\begin{aligned}
 PM_4 &= V_{13} - L_{31} - D \\
 X_{M4,i}PM_4 &= Y_{13,i}V_{13} - X_{31,i}L_{31} - X_{D,i}D \\
 PM_5 &= F - D - B - PM_4 \\
 X_{M5,j}PM_5 &= Z_iF - X_{D,i}D - X_{B,i}B - X_{M4,i}PM_4 \\
 V_2 &= V_1 \\
 L_2 &= L_1 + F \\
 V_3 &= V_4 + V_{13} \\
 L_3 &= L_4 + L_{31} \\
 V_2 &= V_{62}; L_2 = L_{26}; V_4 = V_{44}; \\
 V_6 &= V_5 + V_{62} \\
 L_6 &= L_5 + L_{26} \\
 L_4 &= V_{44} + PM_4 \\
 V_5 &= L_{55} + PM_5 \\
 V_1 &= V_{13}; L_1 = L_{31}; \\
 L_5 &= V_{55} \\
 \Sigma X_i &= \Sigma Y_i = 1
 \end{aligned}$$

FIG. 2. Material balance equations for Configuration 4 (Fig. 1d).

gradients. The method is efficient and widely used for multivariable constrained problems. The algorithm is shown in Fig. 3.

Considering Configuration 1, there are 43 variables and 28 equations describing the model. Therefore, by specifying 15 variables, the others can be calculated. In the problem statement, often the feed rate, its composition, and the product recoveries have been decided; thus, only six variables are left to specify. This is a six-dimensional optimization problem. The objective is to minimize the total cost of the distillation configuration; that is, the sum of the investment cost and the operating cost.

In order to have a feasible result, the basic equation

$$\text{total cost} = \text{annual operating cost} + \frac{\text{investment cost}}{\text{project life}} \quad (8)$$

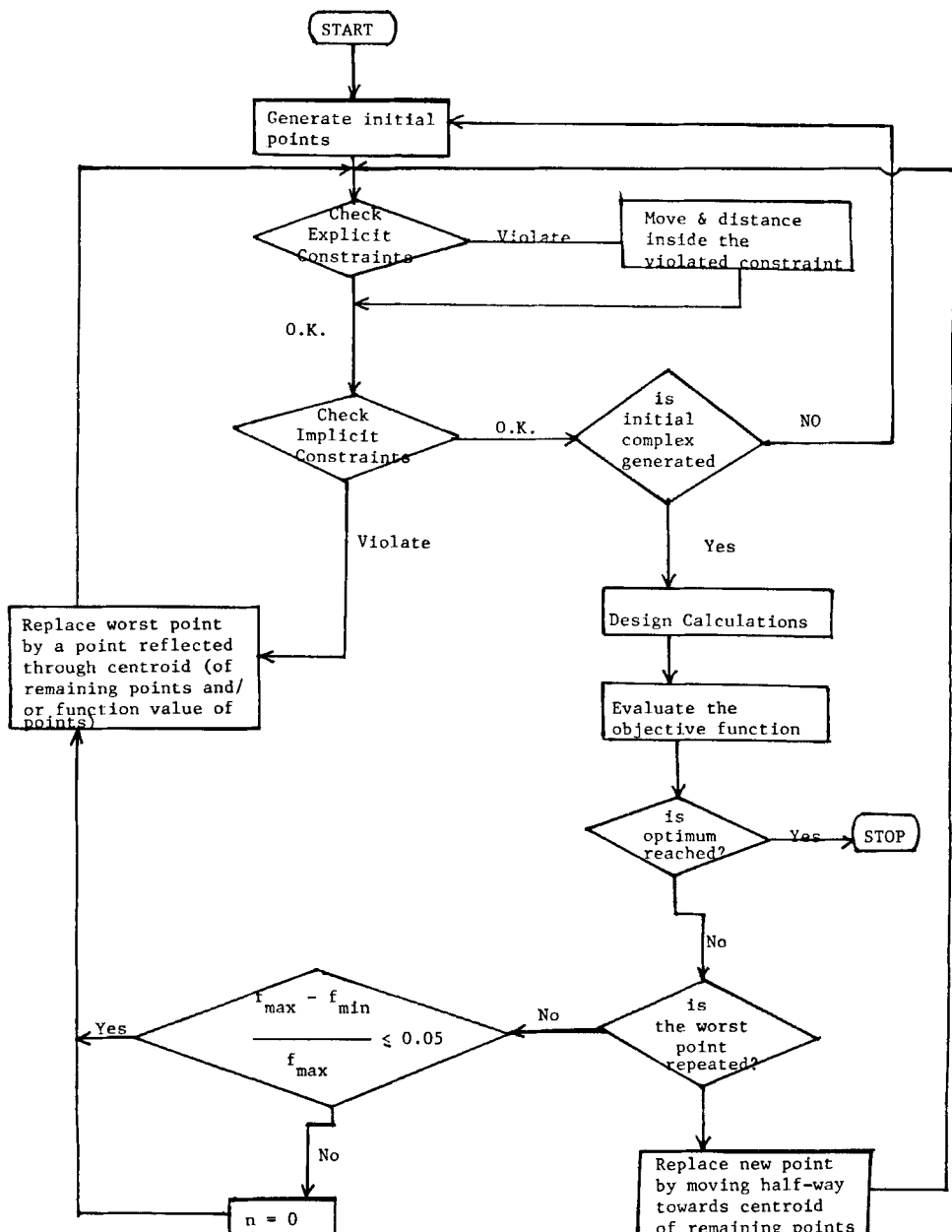


FIG. 3. Flow chart of modified complex method for optimization.

has to be optimized subject to the following constraints on the reflux or reboiler ratios:

$$R_{\max} > R = \frac{L}{D} > R_{\min} \quad (9)$$

$$R'_{\max} > R = \frac{\bar{L}}{B} > R'_{\min} \quad (10)$$

Expressing Eqs. (9) and (10) in terms of liquid and vapor ratio, we have

$$1 > \frac{L}{V} > \frac{R_{\min}}{R_{\min} + 1} \quad (11)$$

$$1 > \frac{\bar{V}}{\bar{L}} > \frac{R'_{\min}}{R'_{\min} + 1} \quad (12)$$

where R_{\min} is the minimum reflux ratio and R'_{\min} is the minimum reboiler ratio.

The minimum reflux ratio can be determined as follows:

(1) For *sharp-separation cases*, the Underwood equations (17) can be used to calculate the minimum reflux ratios as follows:

$$1 - q = \sum \frac{\alpha_i Z_i}{\alpha_i - \theta} \quad (13)$$

$$R_{\min} = \sum \frac{\alpha_i X_{D,i}}{\alpha_i - \theta} - 1 \quad (14)$$

$$R'_{\min} = 1 - \sum \frac{\alpha_i X_{B,i}}{\alpha_i - \theta} \quad (15)$$

These equations can be solved for θ by using the secant method as follows:

$$f(\theta) = -(1 - q) + \sum \frac{\alpha_i Z_i}{\alpha_i - \theta} = 0 \quad (16)$$

$$\theta_{k+1} = \theta_k + \Delta\theta_K \quad (17)$$

$$\Delta\theta_k = - \frac{f(\theta_k)}{\frac{f(\theta_k) - f(\theta_{k-1})}{\theta_k - \theta_{k-1}}} \quad (18)$$

where k is the k th trial.

The value of θ is substituted into Eq. (14) and/or (15) to obtain R_{\min} and/or R'_{\min} .

The following modifications are applied when relative volatilities are not constant as assumed in the Underwood equations. Choose the reference component, usually the heavy key, then calculate the relative volatilities as

$$\alpha_{ir} = K_i/K_r, \quad (19)$$

$$(\alpha_{ir})_{\text{avg}} = [(\alpha_{ir})_{\text{dist}}(\alpha_{ir})_{\text{bott}}(\alpha_{ir})_{\text{feed}}]^{1/3} \quad (20)$$

where avg is the average value, dist is the distillate product, and bott is the bottom product. Use $(\alpha_{ir})_{\text{avg}}$ instead of α_i in Eqs. (13), (14), and (15) to calculate R_{\min} and R'_{\min} .

(2) For nonsharp-separation cases, the Petlyuk et al. (2) method is found accurate and convenient. The method is analytical, and the equations are:

$$R_{\min} = \frac{L_m}{D} = \frac{L_m}{V_m - L_m} \quad (21)$$

$$L_m = \left(\frac{\alpha_{LK}}{\alpha_{LK} - \alpha_{HK}} \right) \left[\frac{q(\Sigma \alpha_i Z_i) + (1 - q)\alpha_{LK}}{\Sigma \alpha_i Z_i} \right] \quad (22)$$

$$V_m = \frac{q(\Sigma \alpha_i Z_i) + (1 - q)\alpha_{LK}}{\alpha_{LK} - \alpha_{HK}} \quad (23)$$

where LK is the lightest component and HK is the heaviest component.

Solution Procedure

The solution procedure is outlined as follows:

1. The independent variables L_{11} , V_{44} , L_{55} , P_1 , P_2 , and P_3 are generated.

This selection is made such that the values are compatible with the constraints, like the minimum reflux ratio, etc.

2. Calculate Y_{13} 's and X_{26} 's from the distribution calculation of non-sharp separation cases.
3. Calculate V_{13} and L_{26} .
4. Calculate X_D , X_B , X_{M4} , and X_{M5} from the distribution calculation method for sharp separation cases.
5. Calculate all flow rates D , B , PM_4 , and PM_5 .
6. Check the feasible conditions for the reflux ratios. If not satisfied, make correction or repeat from Step 1. This action is governed by the optimization method (see Fig. 3).
7. Calculate all internal flows L_1 , V_1 , ..., etc.
8. Calculate the number of stages using stage by stage calculation method.
9. Calculate the reboiler and condenser duties.
10. Calculate the cost.
11. If the minimum objective function value is not reached, return to Step 1 or make the corrections according to the optimization method as previously discussed (see Fig. 3). This step is repeated until the optimum is found. The procedure has to be repeated from several initial values of the independent variables chosen in Step 1 to ensure that the optimum is a global optimum.

The above procedure is general for all configurations. However, the determination of variables should be appropriate to the configuration in question.

Finally, for Configurations 2 and 3, additional steps are needed to determine X_{45} 's, Y_{54} 's, and X_{M4} 's as follows:

- 4a. Use the Gauss Jordan technique to solve the simultaneous equations below:

$$X_{45,i}(PM_4 + L_{45}) - Y_{54,i}V_{54} = Y_{13,i}V_{13} - X_{D,i}D, \quad i = 1, \dots, 3 \quad (24)$$

$$Y_{54,i}V_{54} - X_{45,i}L_{45} = L_{26}X_{26,i} - BX_{B,i}, \quad i = 1, \dots, 3 \quad (25)$$

- 4b. And $X_{M4,i} = X_{45,i}$.

For Configurations 5, 6, 7, and 8, Step 2 is not needed.

The optimization variables for each configuration are summarized in Table 4.

TABLE 4
Optimization Variables for the Eight Configurations

Configuration	Optimization function
1	$f(L_{11}, V_{44}, L_{55}, P_1, P_2, P_3)$
2	$f(L_{11}, L_{45}, P_1)$
3	$f(V_{13}, L_{45}, P_1)$
4	$f(V_{13}, V_{44}, L_{55}, P_1)$
5	$f(L_{11}, L_{33}, P_1, P_2)$
6	$f(L_{11}, L_{33}, P_1, P_2)$
7	$f(L_{11}, L_{33}, P_1)$
8	$f(L_{13}, L_{33}, P_1)$

RESULTS AND DISCUSSIONS

The minimum total cost of the configurations was obtained for separating a ternary mixture with 99% recovery of the components. Various feed compositions were studied. The results are listed in Table 5. Four typical plots of the unit cost (ratio of the minimum cost to the feed rate) versus the mole fractions are shown in Figs. 4 to 7.

Figure 4 shows the case where there is small amount of the lightest

TABLE 5
Unit Optimal Costs of the Eight Configurations for Different Feed Compositions

Feed composition (<i>n</i> -C ₅ , <i>n</i> -C ₆ , <i>n</i> -C ₇)	Unit cost of configuration ($\times 10^{-2}$ \$/kg · mol of feed) for configuration							
	1	2	3	4	5	6	7	8
0.10, 0.10, 0.80	3.18	3.08	2.51	2.82	4.34	3.55	2.69	4.34
0.45, 0.10, 0.45	3.46	3.85	2.56	3.05	4.83	4.15	2.80	3.99
0.50, 0.10, 0.40	3.47	4.21	2.76	3.06	4.58	4.23	2.94	3.96
0.70, 0.10, 0.20	3.83	6.28	4.53	3.44	4.75	4.66	3.84	3.36
0.80, 0.10, 0.10	3.77	—	7.74	3.80	3.74	5.08	—	3.70
0.10, 0.45, 0.45	3.79	3.54	3.02	3.84	5.01	3.83	3.99	5.15
0.10, 0.60, 0.30	4.47	3.90	—	5.30	4.89	4.05	5.18	4.39
0.10, 0.70, 0.20	4.87	4.24	3.78	—	4.38	4.48	6.50	4.83
0.10, 0.80, 0.10	6.02	4.55	3.83	6.71	4.87	4.62	—	5.00
0.40, 0.20, 0.40	3.62	3.61	2.87	3.22	4.78	4.07	3.27	4.19
0.33, 0.34, 0.33	3.74	3.77	3.17	3.79	3.87	4.11	4.16	4.59
0.20, 0.60, 0.20	—	4.32	3.57	4.76	4.34	4.79	6.01	4.59
0.45, 0.45, 0.10	4.62	5.43	5.53	5.56	4.11	5.05	—	4.95
0.30, 0.40, 0.30	3.94	3.92	3.23	4.01	3.77	4.24	4.39	4.12
0.70, 0.20, 0.10	3.88	7.82	6.45	4.40	3.80	5.23	—	4.12

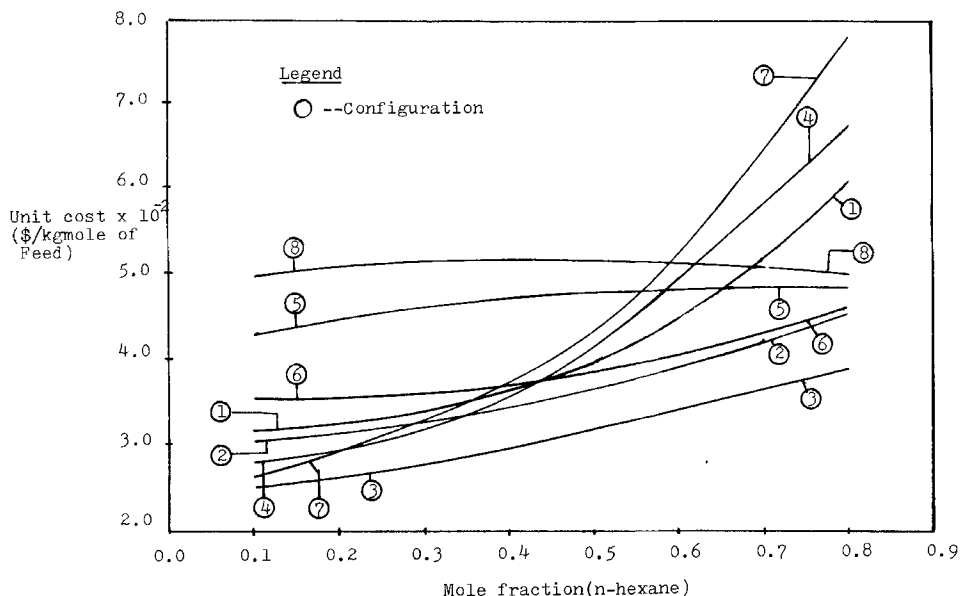


FIG. 4. Unit cost vs mole fraction *n*-hexane when *n*-pentane mole fraction = 0.1.

component (*n*-pentane) present in the feed. The unit cost was plotted versus the mole fractions of the middle component (*n*-hexane). It suggests that for Configurations 1, 4, and 7 the cost increases significantly with increasing amounts of the middle component. Also, Configuration 3 is optimum over the whole range of *n*-hexane mole fractions. Figure 5 shows a plot of the unit cost versus the mole fraction of *n*-hexane when small amounts of the heaviest component (*n*-heptane) are present in the feed. As expected, the results for Configurations 1 and 4 remain unchanged. However, for Configurations 2, 3, 5, and 6, opposite trends were observed. Relative to other configurations, Configuration 5 is economical when the *n*-hexane mole fraction is smaller than 0.6; otherwise, Configuration 3 is favored.

For equimolar amounts of the lightest and heaviest component in the feed, a plot of unit cost versus the mole fraction of the middle component is shown in Fig. 6. The results for Configurations 1, 4, and 7 remain unchanged. The optimum for Configurations 5 and 6 was obtained at *n*-hexane mole fractions of 0.35 and 0.25, respectively. Relative to other configurations, Configuration 3 was better throughout the entire range of *n*-hexane mole fractions.

As shown in Fig. 7, the unit cost of Configurations 2 and 3 increases

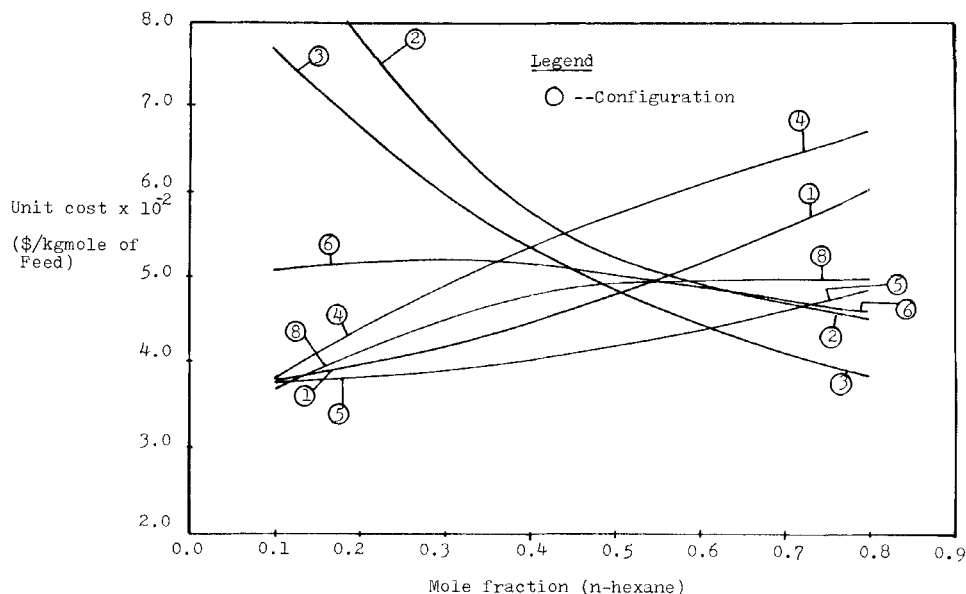


FIG. 5. Unit cost vs mole fraction *n*-hexane when *n*-heptane mole fraction = 0.1.

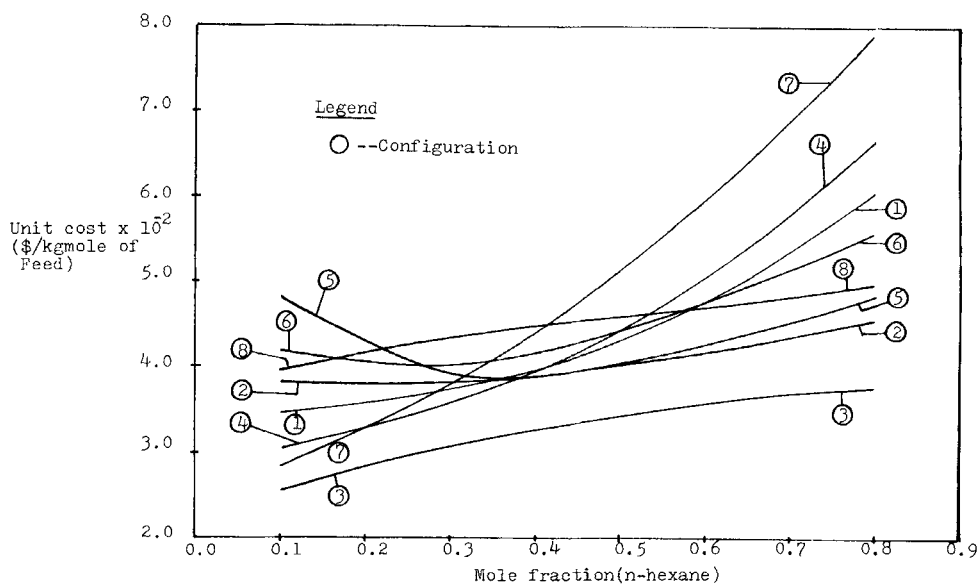


FIG. 6. Unit cost vs mole fraction *n*-hexane for equimolar amounts of *n*-pentane and *n*-heptane.

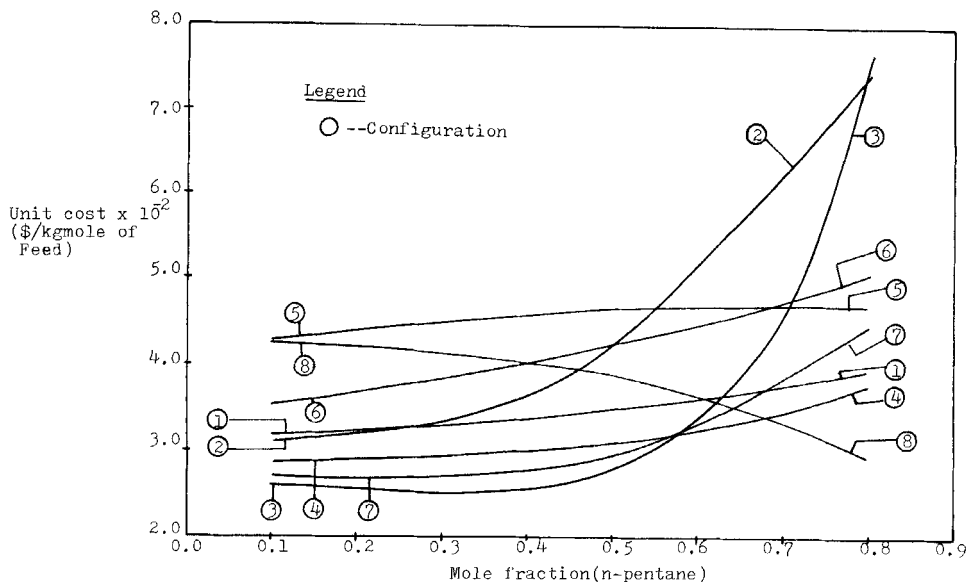


FIG. 7. Unit cost vs mole fraction *n*-pentane when *n*-hexane mole fraction = 0.1.

significantly as the lightest component (*n*-pentane) mole fraction increases. This happens when a small amount of the middle component (*n*-hexane) is present in the feed. For *n*-pentane mole fractions less than 0.57, Configuration 3 is cheaper compared to the other configurations. For Configuration 8, the unit cost decreases as the mole fraction of *n*-pentane increases and the configuration becomes cheaper for *n*-pentane mole fractions greater than 0.7. For values of *n*-pentane mole fraction between 0.57 and 0.7, Configuration 4 is cheaper compared to the other configurations.

Figures 8 to 22 summarize the optimal regions for all the configurations. Figure 8 presents the optimum region for Configurations 1 and 2. For both these configurations the overhead product rate and the middle product rate can be varied over a wide optimization range. Thus, they usually obey the rule "favor equimolar splits" suggested by Harbert (18). In addition, in these configurations the easiest separation is performed first, i.e., the lightest/heaviest component separation precedes the more difficult lightest/middle component separation. However, despite these advantages, Configuration 1 is more expensive at Composition II. This is mainly due to the expensive downstream columns caused by large vapor rate requirements in Columns 2 and 3. It is evident from Figs. 4 to 7 that

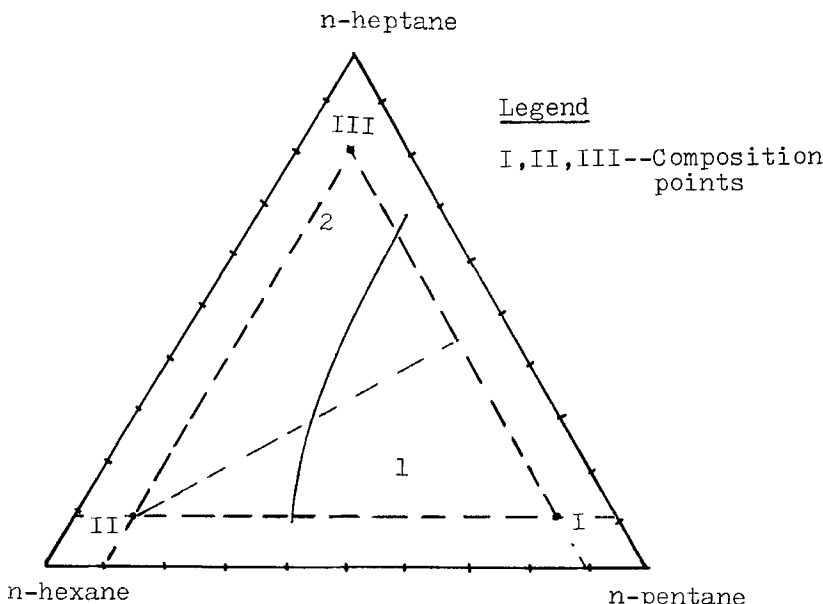


FIG. 8. Regional optimum of Configurations 1 and 2.

the minimum cost of Configuration 1 increases significantly as the middle product rate increases.

At Composition II, Configuration 2 is cheaper than Configuration 1. This is due to the thermal coupling between Columns 2 and 3 of Configuration 2 which minimizes the vapor rate in the system. Due to the withdrawal of the middle product from the liquid reflux of Sections 5 and 6, the large vapor requirement of these sections is avoided.

Tedder and Rudd (5) concluded that Configurations 1 and 2 were comparable in costs over almost the entire range of feed compositions. This is supported by Munoz and Seader (6) who used a thermodynamic objective function.

Figure 9 shows the optimal region for Configurations 3 and 4. The relative costs between Configurations 3 and 4 are determined by the same factors which lead to the differences between Configurations 1 and 2.

The effect of thermal coupling can be seen from Figs. 10 and 11. Configuration 4 appears cheaper than Configuration 1 for compositions along the Line I-III, and also in the region where a large bottom product has to be produced (Fig. 10). This is due to thermal coupling between the columns, i.e., the unfavorable feed conditions to the downstream

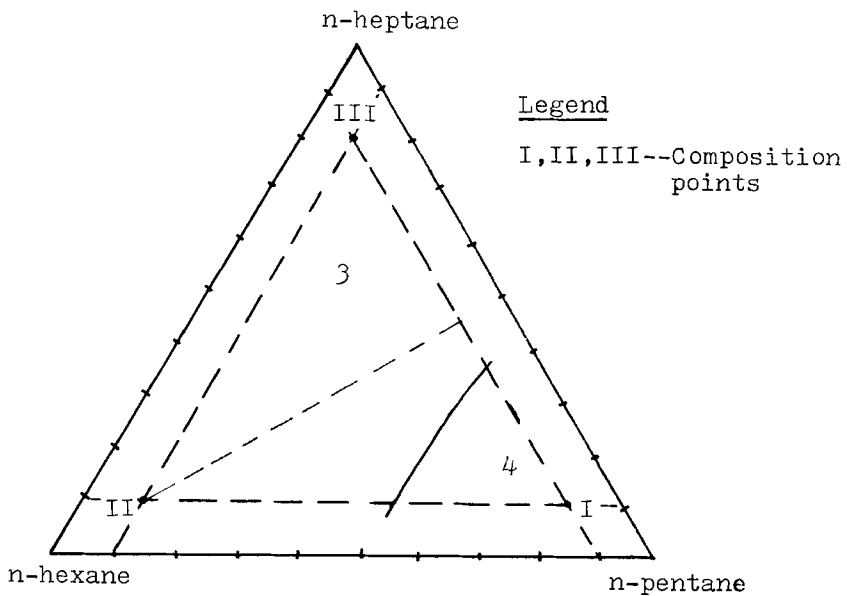


FIG. 9. Regional optimum of Configurations 3 and 4.

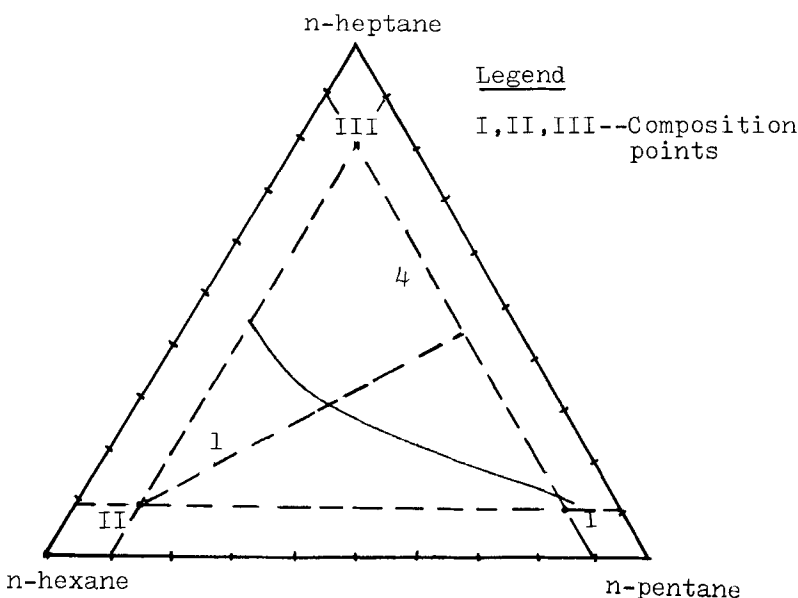


FIG. 10. Regional optimum of Configurations 1 and 4.

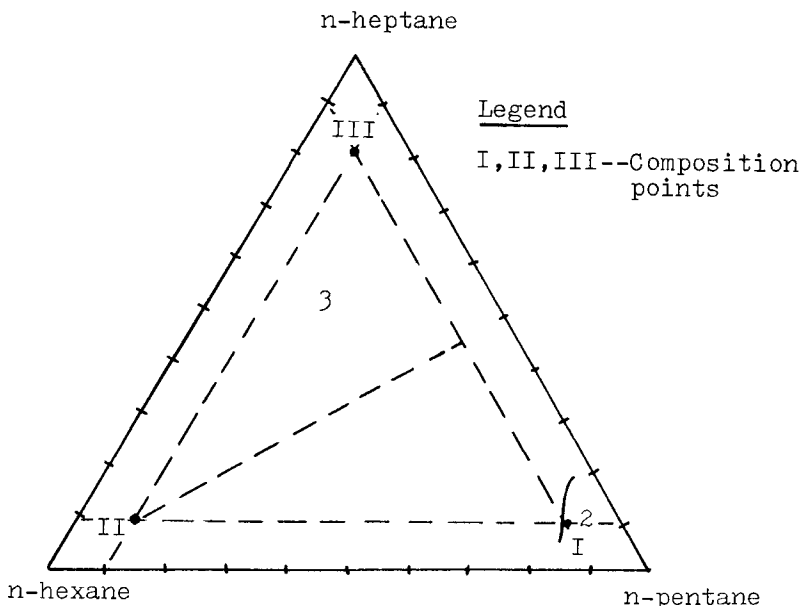


FIG. 11. Regional optimum of Configurations 2 and 3.

columns (Columns 2 and 3) as in Configuration 1 can now be optimized to minimize the total vapor requirement of the system. However, when the middle product rate increases, a higher vapor rate is required in Column 3 to supply vapor to Column 1. This makes Configuration 4 more expensive than Configuration 1. Similarly, as can be seen in Fig. 11, Configuration 3 is cheaper than Configuration 2.

Figure 12 defines the optimum region for Configurations 5 and 6. Configuration 6 is cheaper than Configuration 5 when the amount of bottom product is large. The reverse happens when a large quantity of overhead product is needed. This has been examined by Rod and Marek (19) and Tedder and Rudd (5). In the dashed region shown in Fig. 12, Configurations 5 and 6 are comparable (5). The general trends for the defined regions have been verified by other authors (6, 7).

This study agrees with the heuristic "favor the direct sequence when equimolar amounts of components with equal relative volatilities are present in feed," suggested by Nishimura et al. (20).

Comparing Configurations 5 and 7 and 6 and 8 when small amounts of overhead product are produced, Configuration 7 is cheaper relative to Configuration 8. This occurs because the required vapor rate in Column 1 and Column 2 (Configuration 7) is small. Both Configurations 7 and 8

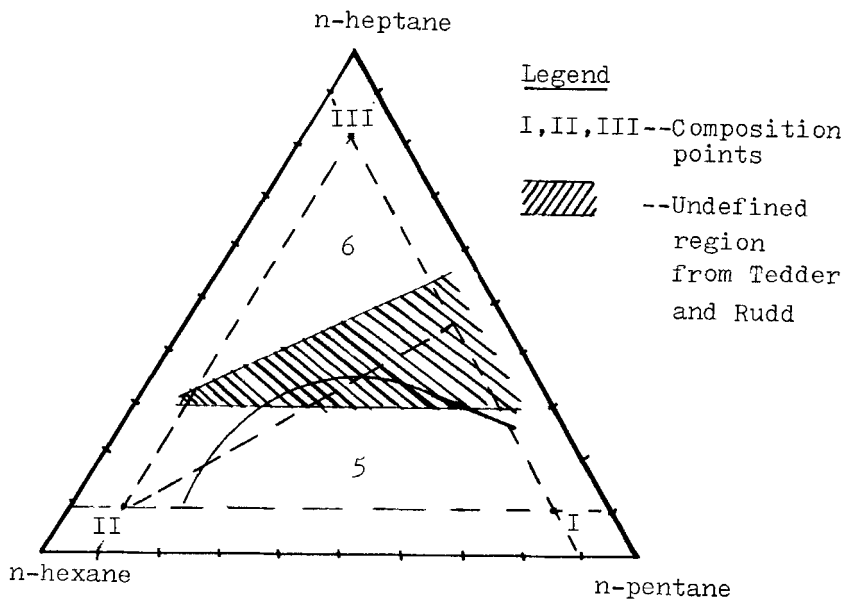


FIG. 12. Regional optimum of Configurations 5 and 6.

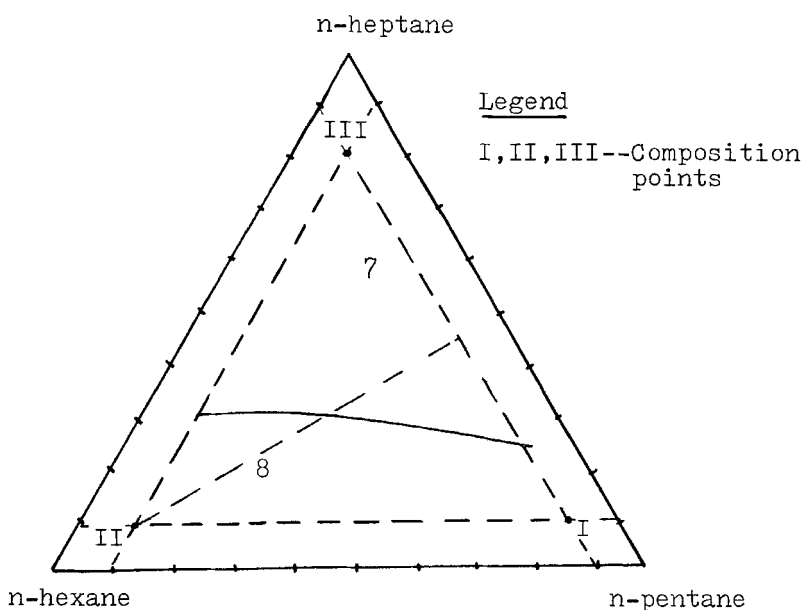


FIG. 13. Regional optimum of Configurations 7 and 8.

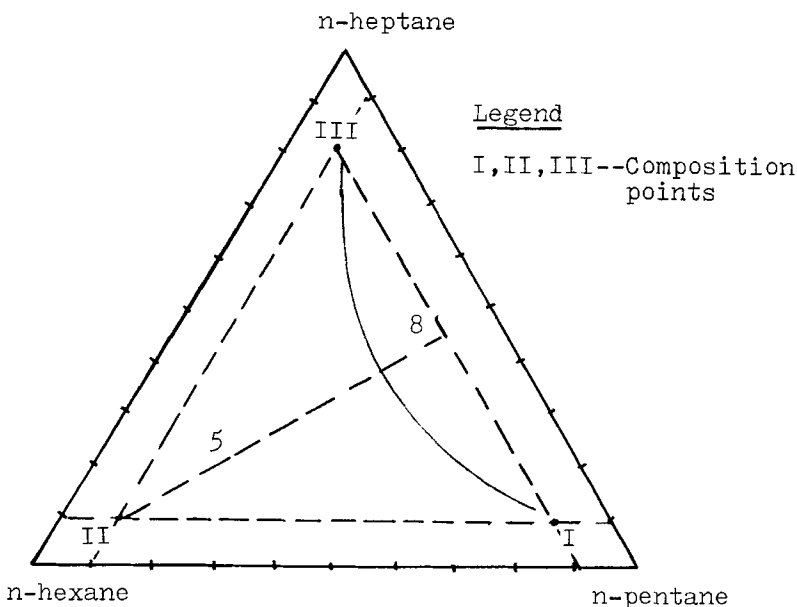


FIG. 14. Regional optimum of Configurations 5 and 8.

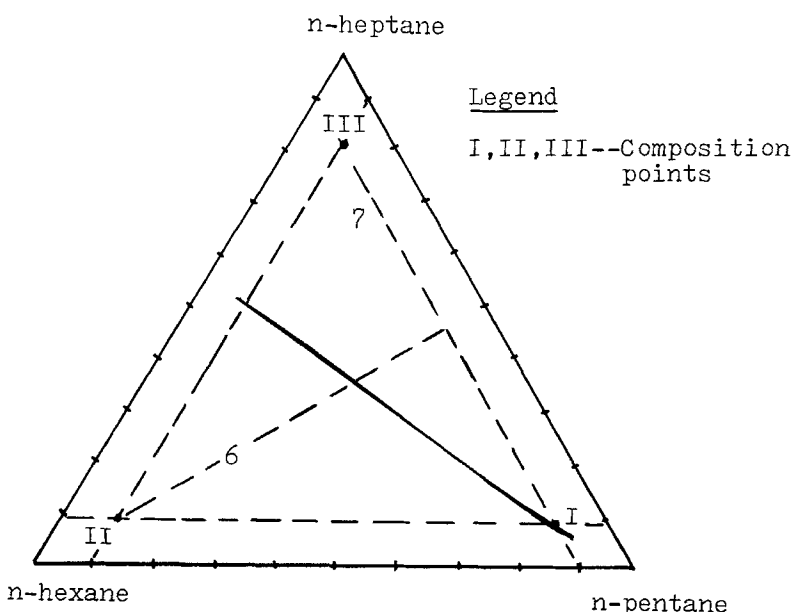


FIG. 15. Regional optimum of Configurations 6 and 7.

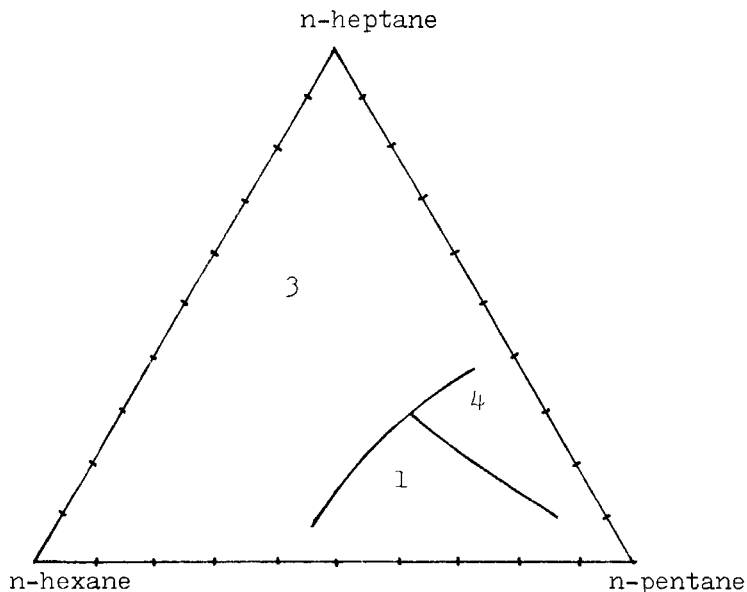


FIG. 16. Regional optimum of Configurations 1, 2, 3, and 4.

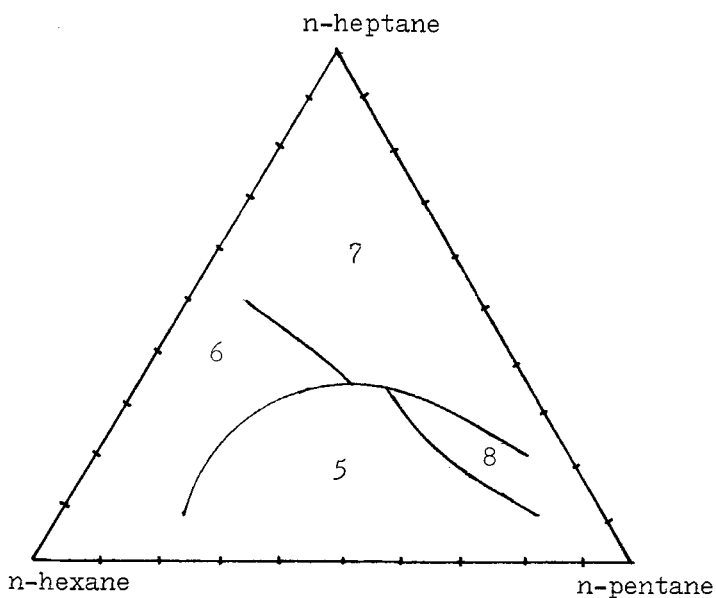


FIG. 17. Regional optimum of Configurations 5, 6, 7, and 8.

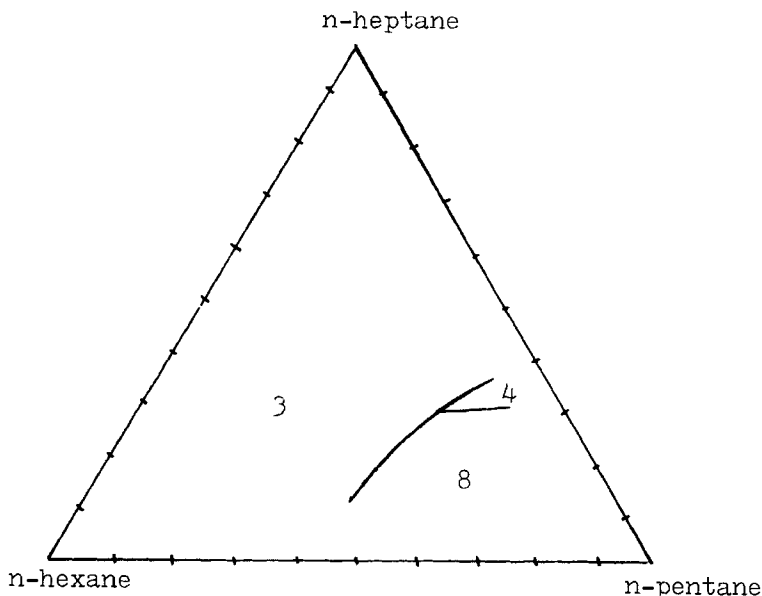


FIG. 18. Regional optimum of Configurations 3, 4, 7, and 8.

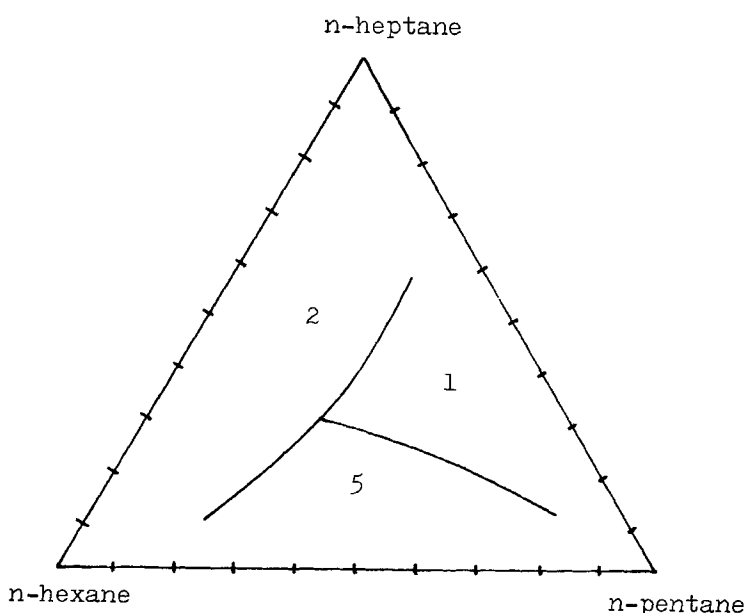


FIG. 19. Regional optimum of Configurations 1, 2, 5, and 6.

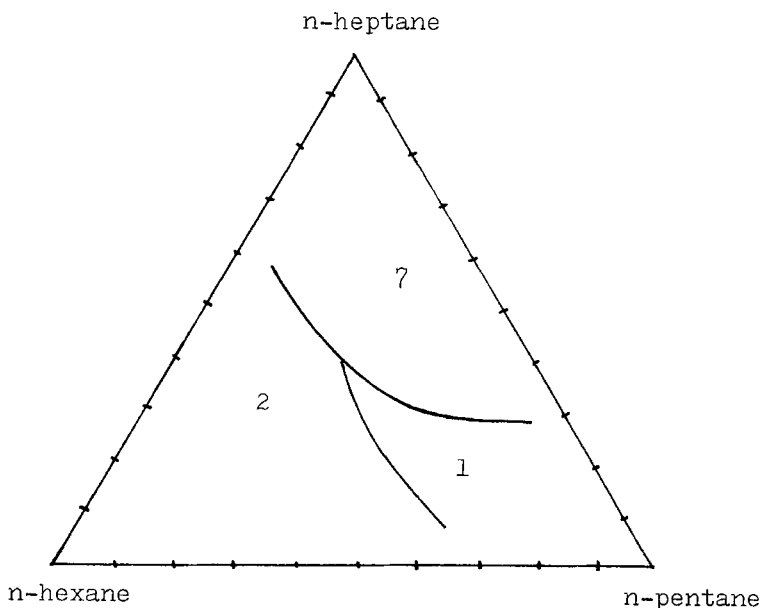


FIG. 20. Regional optimum of Configurations 1, 2, 7, and 8.

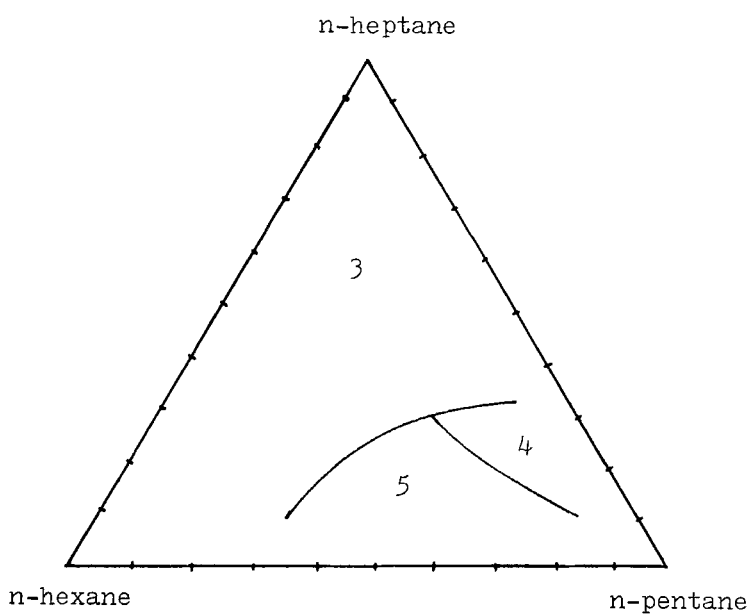


FIG. 21. Regional optimum of configurations 3, 4, 5, and 6.

appear attractive for compositions along the Line I-III. The greatest advantage of Configuration 8 relative to Configuration 5 is at Composition IV. At this composition, both columns in Configuration 5 are large, whereas Column 2 in Configuration 8 is small. Similarly, Configuration 7 is cheaper than Configuration 6 at Composition III.

Tedder and Rudd (5) and Munoz and Seader (6) compared Configurations 1, 5, 6 and also 2, 5, 6. They found that both Configurations 1 and 2 were cheaper than Configurations 5 and 6 if the feed contained an appreciable amount of the middle component (B) and the difference increased as the amount of B in the feed increased. This study supports these findings for Configurations 2, 5, and 6 but not for Configurations 1, 5, and 6.

Fidkowski and Krolkowski (7) also found that among Configurations 2, 3, 5, and 6, Configuration 3 was the cheapest over all feed compositions. This study shows that Configuration 3 is cheaper than Configurations 2, 5, and 6 for all feed compositions except when the lightest component (A) is present in large quantities in the feed. When this happens, the direct sequence (Configuration 5) is the cheapest followed by the indirect sequence (Configuration 6).

CONCLUSIONS

Eight configurations consisting of conventional, complex, and thermally coupled types have been studied. Their characteristics and advantages have been explored and the optimal regions are summarized in Figs. 15 to 20. The overall conclusions when all configurations are considered (Fig. 22) can be summarized as follows:

1. Configuration 5 is favorable if less than 30% bottom product, more than 35% overhead product, and more than 15% middle product are present in the feed.
2. Configuration 8 is favorable if less than 35% bottom product and less than 15% middle product are present in the feed.
3. Otherwise, favor Configuration 3.

For a specific feed composition, the precise optimal configuration can be found from Fig. 22.

SYMBOLS

A_1, A_2, A_3

Antoine's constants

B

bottom product flow rate ($\text{kg} \cdot \text{mol}/\text{h}$)

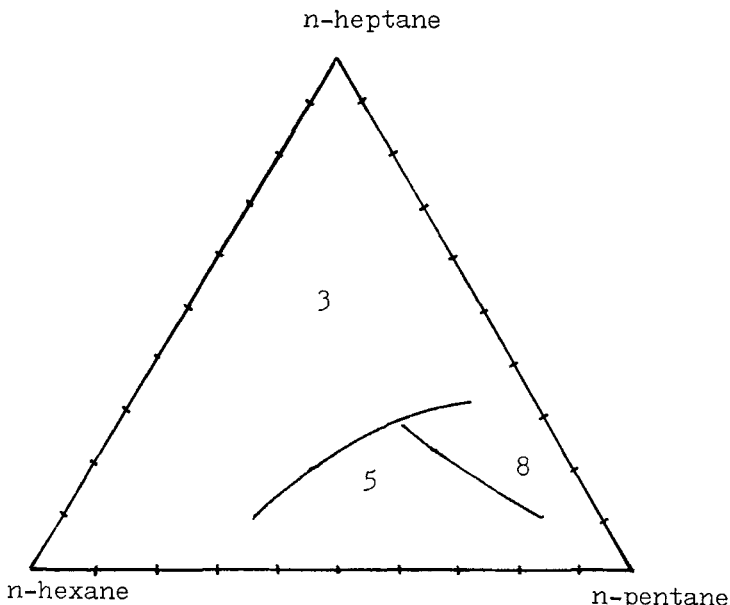


FIG. 22. Regional optimum of Configurations 1, 2, 3, 4, 5, 6, 7, and 8.

b	component flow rate in bottom product (kg · mol/h)
C_1, C_2	correlation constants of component distribution equation
D	distillate product flow rate (kg · mol/h)
d	component flow rate in distillate product (kg · mol/h)
d_0, d_1, d_2, d_3, d_4	correlation constants in vapor enthalpy calculation
e_0, e_1, e_2	correlation constants in liquid enthalpy calculation
F	feed flow rate (kg · mol/h)
f	component flow rate in feed (kg · mol/h)
H	vapor enthalpy (kcal/kg · mol)
h	liquid enthalpy (kcal/kg · mol)
K	equilibrium constant
L	liquid rate in rectifying section (kg · mol/h)
L_m	minimum liquid rate in rectifying section (kg · mol/h)
\bar{L}	liquid rate in stripping section (kg · mol/h)
N	total number of components in feed
PM_4, PM_5	middle product rate, withdrawn from Sections 4 and 5 (kg · mol/h)
P^o	vapor pressure (atm)
P_1, P_2, P_3	operating pressure of Columns 1, 2, and 3 (atm)

q	fraction of liquid in feed
R	reflux ratio
R_{\min}	minimum reflux ratio
R'_{\min}	minimum reboiler ratio
T	temperature (°K)
V	vapor rate of rectifying section (kg · mol/h)
V_m	minimum vapor rate in rectifying section (kg · mol/h)
\bar{V}	vapor rate in stripping section (kg · mol/h)
X	liquid mole fraction
X_B	mole fraction of bottom product
X_D	mole fraction of top product
Y	vapor mole fraction
Z	feed mole fraction

Greek Letters

α	relative volatility
δ	correction factor
η	degree of tray efficiency
θ	parameter in Underwood equation

Subscripts and Superscripts

avg	the average value
i	the component i ; $i = 1, 2, \dots, N$
K	the K th trial in the trial-and-error process
strip	the value in the stripping section
rect	the value in the rectifying section

REFERENCES

1. N. Nishida, G. Stephanopoulos, and A. W. Westerberg, "A Review of Process Synthesis," *AIChE J.*, 27, 321 (1980).
2. F. B. Petlyuk, V. M. Platonov, and D. M. Slavinskii, "Thermodynamically Optimum Method for Separating Multicomponent Mixtures," *Int. Chem. Eng.*, 5(3), 555 (1965).
3. W. J. Stupin and F. J. Lockhart, "Thermally Coupled Distillation—A Case History," *Chem. Eng. Prog.*, 68(10), 71 (1972).
4. N. Doukas and W. L. Luyben, "Economics of Alternative Distillation Configurations for the Separation of Ternary Mixtures," *Ind. Eng. Chem., Process Des. Dev.*, 17, 272 (1978).
5. D. W. Tedder and D. F. Rudd, "Parametric Studies in Industrial Distillation," *AIChE J.*, 24(2), 303 (1978).

6. A. G. Munoz and J. D. Seader, "Synthesis of Distillation Trains by Thermodynamic Analysis," *Comput. Chem. Eng.*, 2(4), 311 (1985).
7. Z. Fidkowski and L. Krolkowski, "Thermally Coupled System of Distillation Columns: Optimization Procedure," *AIChE J.*, 32(4), 537 (1986).
8. E. R. Gillian and C. E. Reed, "Degrees of Freedom in Multicomponent Absorption and Rectification Columns," *Ind. Eng. Chem.*, 34, 551 (1942).
9. C. L. Yaws, P. M. Patel, F. H. Pitts, and C. S. Fang, "Estimate Multicomponent Recover," *Hydrocarbon Process.*, p. 99 (February 1979).
10. R. J. Hengstebeck, *Trans. AIChE*, 42, 309 (1948).
11. R. L. Geddes, *AIChE J.*, 4, 389 (1958).
12. R. N. S. Rathore, K. A. V. Wormer, and G. J. Powers, "Synthesis Strategies for Multicomponent Separation Systems with Energy Integration," *AIChE J.*, 20(3), 491 (1974).
13. K. M. Guthrie, "Capital Cost Estimating," *Chem. Eng.*, p. 114 (March 1969).
14. J. B. Maxwell, *Data Book on Hydrocarbons*, Van Nostrand, New York, 1950.
15. E. J. Henley and J. D. Seader, *Equilibrium Stage Separation Operations in Chemical Engineering*, Wiley, New York, 1981.
16. T. Umeda and A. Ichikawa, "A Modified Complex Method for Optimization," *Ind. Eng. Chem., Process Des. Dev.*, 10, 236 (1971).
17. A. I. V. Underwood, *Chem. Eng. Prog.*, 44, 603 (1948).
18. W. D. Harbert, "Which Tower Goes Where?" *Pet. Refiner.* 36(3), 169 (1957).
19. V. Rod and J. Marek, "Separation Sequences in Multicomponent Rectification," *Collect. Czech. Chem. Commun.*, 24, 3240 (1959).
20. H. Nishimura and Y. Hiraizumi, "Optimal System Pattern for Multicomponent Distillation Systems," *Int. Chem. Eng.*, 11(1), 188 (1971).

Received by editor July 2, 1986

Revised October 20, 1986